

USE OF MACHINE LEARNING ALGORITHMS TO CLASSIFY ANOMALIES IN CLOSED COAL COMBUSTION RESIDUALS DISPOSAL SITES

Hanlei Gu¹, Wladimiro Villarroel¹, Benjamin Gallagher², Brian Palmer³

¹The Ohio State University, Department of Electrical and Computer Engineering; ² Electric Power Research Institute; ³ American Electric Power

KEYWORDS: machine learning, coal ash, fly ash, CCR, disposal sites

ABSTRACT

The disposal of Coal Combustion Residuals (CCR) is typically managed in landfills or ponds. Closure of these units involves construction of an engineered barrier system aimed at protecting the CCR from exposure to the environment. Engineered barriers commonly consist of multiple layers of different materials, including soil and synthetics. Over time a protective cover might be compromised by a plurality of external factors, increasing the risk of exposure of CCR to the environment. These factors include animal activity, climate effects, and ground movement, which may wear, erode, create voids, or unlevel the terrain ultimately affecting the integrity of the cover. In this paper, the results of using a Ground Penetrating Radar (GPR) to inspect the protective cover of a CCR landfill for detecting and classifying the presence of certain anomalies are presented¹. The anomalies are intentionally buried in the protective layer and are representative of typical issues encountered in the field, such as animal burrows, voids, and water accumulation¹. GPR data are further processed using customized machine learning algorithms developed to improve the classification accuracy of anomalies¹. The goal is to detect the presence of anomalies, identify their location in the field, and classify the type of anomaly detected to provide the appropriate information for warning and taking the corresponding actions to deal with the potentially compromised region of the protective layer, significantly reducing the risk of CCR exposure. Eventually, the GPR-based system might be implemented in a motorized ground vehicle or an unmanned aerial vehicle for more effectively monitoring extensive land areas.

INTRODUCTION

Fly ash is a common CCR consisting of the fine, non-combustible minerals contained coal. Fly ash contains a range of trace elements, including constituents like arsenic, that originated in the coal. Improper disposal of CCR can result mobilization of trace elements and contamination of the environment. Environmental regulations dictate closed fly ash landfills be properly capped and inspected to limit the potential for environmental contamination². In particular, the protective multilayer cap systems used in landfill closure require routine inspection and maintenance to maintain performance and avoid degradation by factors like animal activity, climate effects, and ground movement. Different actions need to be taken to address these factors. The use of Non-Destructive Techniques (NDT) is preferred for the inspection of the protective layer of a CCR landfill site. Among the NDTs, Ground Penetrating Radar (GPR) has shown to have advantages over other techniques³.

GPR systems use radiofrequency (RF) pulses to see through the subsurface. The magnitude of the pulses is colored in a grayscale to form a radargram or B-Scan image. This technique is particularly useful in detecting discontinuities in the cap system of closed CCR disposal sites. Figure 1 shows the working principle of GPR⁴.

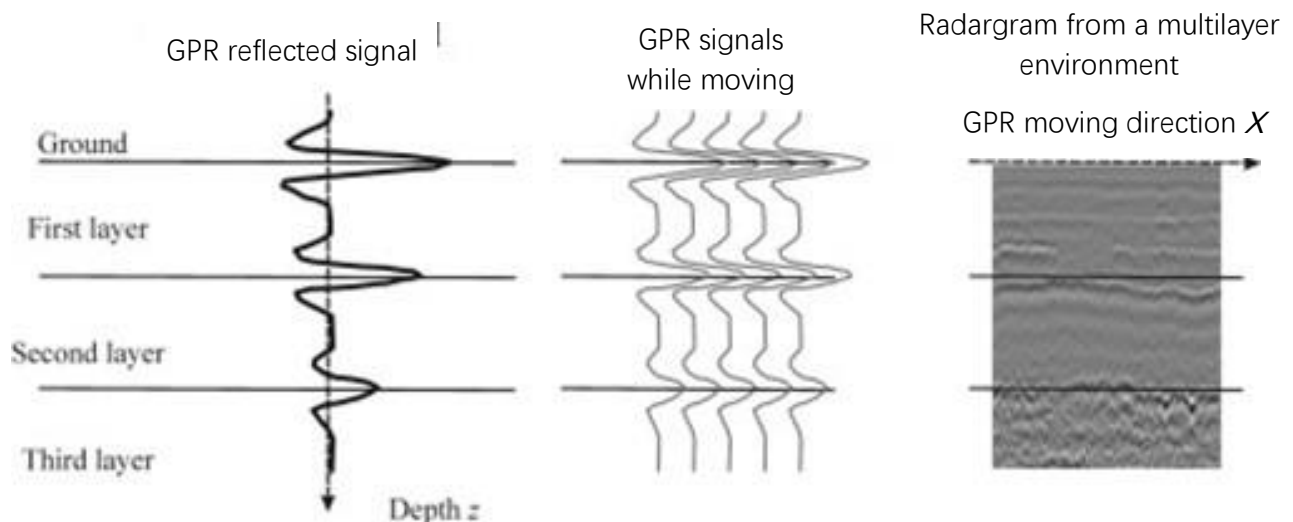


Figure 1. Working Principle of GPR⁴

For maintaining the integrity of the cap system, different actions are required according to the type of compromise in the cover layer. This usually requires a skilled operator to evaluate the situation and determine the compromises found. Machine learning algorithms along with GPR can be used for detecting and predicting or classifying inspection data without the need of a human operator. This streamlines the process and reduce human labor and errors.

EXPERIMENTAL SETUP

The collection of GPR B-Scans is done by manually setting up artificial anomalies underground, and then moving the GPR stepwise across the ground surface over the anomalies while taking measurements

Voids, animal burrows, and water accumulation are three key anomalies of concern in a cap system. To model voids and animal burrows, Styrofoam material is used since it has a similar dielectric permittivity to that of air⁵. Water-on-plastic-film and water bottles are used to model surface water accumulation and underground accumulation, respectively. Figures 2 to 4 show the Styrofoam models used for simulating voids and animal burrows, and a water bottle used for modeling water accumulation.



Figure 2 (Left). Styrofoam used to model a cylindrical void

Figure 3 (Middle). Styrofoam used to model animal burrow

Figure 4 (Right). Water bottle used to model water accumulation

Figure 5 shows sample B-Scans of different anomalies in the experimental setup.

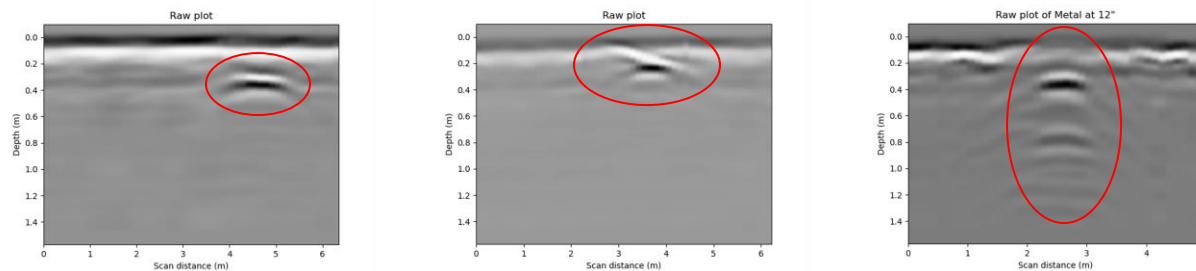


Figure 5. Sample B-Scans

(Left) Sample Void B-Scan. (Middle) Sample animal burrow B-Scan. (Right) Sample water accumulation B-Scan.

Voids show a very clean hyperbolic shape, while animal burrows have a connection from the ground surface to the hyperbola. Water anomalies are the most obvious. Water traps the RF pulse and causes it to reflect several times before fading out. This generates a ringing effect of the hyperbolic shapes after the first reflection.

FIELD TEST

A total of nine anomalies were prepared and buried at different depths in the cap system of an existing fly ash landfill site located in Athens, OH. Figure 6 shows the Cobra GPR module used in the field test. Figure 7 shows group members taking measurements on the landfill site in Athens, OH.



Figure 6 (Left). Cobra GPR module

Figure 7 (Right). Measurement in the field

The dimensions, depth, and corresponding class of each anomaly are recorded in Table 1.

Table 1. Field test anomaly and class

Anomaly	Anomaly class	Depth (m)	Dimensions (m)
aug16_flatvoid3	Void	Z = 0.0762	L = 0.2286; D = 0.1016
aug16_flatvoid9	Void	Z = 0.2286	L = 0.2286; D = 0.1016
aug16_shpere3	Void	Z = 0.0762	D = 0.1524
aug16_void6	Void	Z = 0.1524	L = 0.2032; D = 0.2286
aug16_void12	Void	Z = 0.3048	L = 0.2032; D = 0.2286
aug16_burrow3	Burrow	Z = 0.0762	L = 0.2032; D = 0.2286
aug16_burrow6_surface	Burrow	Z = 0.1524	L = 0.2032; D = 0.2286
aug16_puddle_surface	Water Accumulation	Z = 0	L = 0.0762; D = 0.0762
aug16_puddle3	Water Accumulation	Z = 0.0762	L = 0.21; D = 0.0686

Figure 8 shows a schematic setup for the different anomalies dimension and depth.

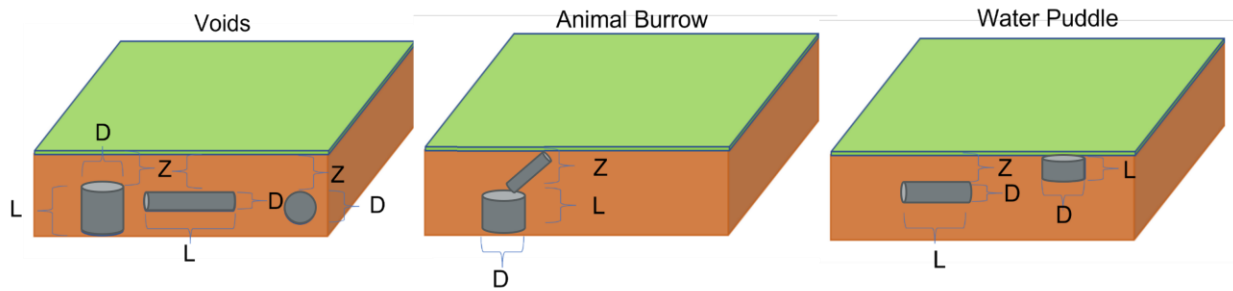


Figure 8. Schematic for void, animal burrow and water puddle

CONVOLUTIONAL NEURAL NETWORK

Convolutional Neural Networks (CNNs) have demonstrated good capabilities to extract spatial features for classification purposes⁶. Given that GPR B-Scans provide depth and distance information, a CNN is proposed as a suitable model for classification of anomalies detected in the cap system. CNN convolves different kernels with each image to extract different spatial information. In particular, CNNs have been successfully applied to detect rebars in wall⁷.

As shown in Figure 5, different classes of anomaly show different structures in B Scan images, which is suitable for image classification using a CNN model.

The CNN model used for the test is implemented using PyTorch framework. The model follows the structure listed in Table 2.

Table 2. CNN model structure

Layer (type)	Output shape
Conv2D	480,640,16
ReLU (Rectified Linear Unit)	480,640,16
MaxPooling2D	240,320,16
Conv2D	240,320,16
ReLU	240,320,16
MaxPooling2D	120,160,16
Linear	512
ReLU	512
Linear	4

Conv2D are layers that convolve the input image with kernels to extract features. ReLU is an activation function used to model the firing of neurons. MaxPooling2D layer helps with reducing the dimensionality of data. Linear layer turns the tensor structure of the data into an array-like manner⁸.

TEST RESULTS

Including several field tests and measurements in a laboratory setup, a total of 112 data samples were collected to implement the CNN model. A set of 70 samples were used for training and 42 samples were used for validation of the model. Then, the CNN model was applied to the results of the field test at the existing fly ash landfill site. Table 3 contains the validation accuracies of the CNN model and other prior Neural Network (NN) models used for anomaly classification, which include NN model with Discrete Wavelet Transform (DWT) and Fractional Fourier Transform (FRFT)⁹ and NN model with Hilbert Transform¹⁰.

Table 3. Classification models and accuracies

Model Name	Validation Accuracy (%)
CNN model with 40x40 input size	88.1 (37 out of 42)
Neural Network with DWT-FRFT Transform	93.75 ⁹
Neural Network with Hilbert Transform	85.71 ¹⁰

In addition, threshold detection and edge detection methods have been used with GPR to detect anomalies in the protective layer^{10,11}. Figures 9 to 17 show the raw B-Scan images (Left), B-Scan images after threshold detection (Middle), and B-Scan images after edge detection (Right). In each B-Scan, potential anomalies are circled in red, and if one actual anomaly is not detected, its location is circled in green.

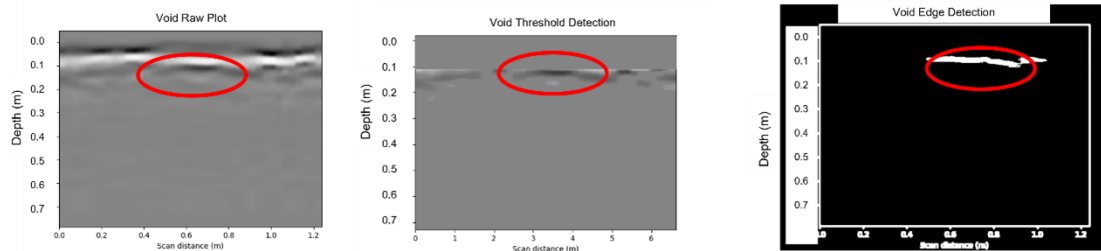


Figure 9. Void anomaly: Aug16_flatvoid3

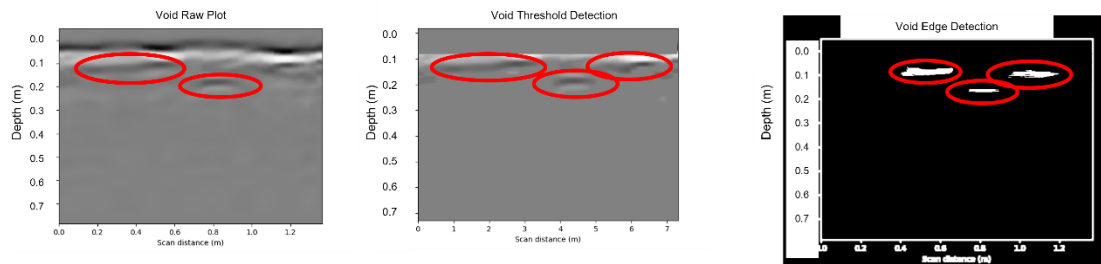


Figure 10. Void anomaly: Aug16_flatvoid9

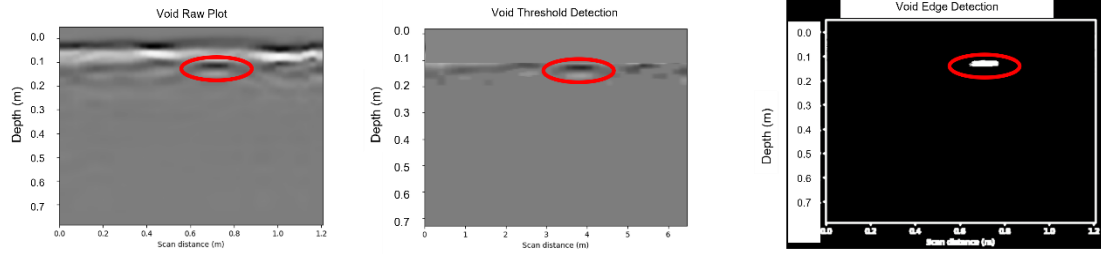


Figure 11. Void anomaly: Aug16_sphere3

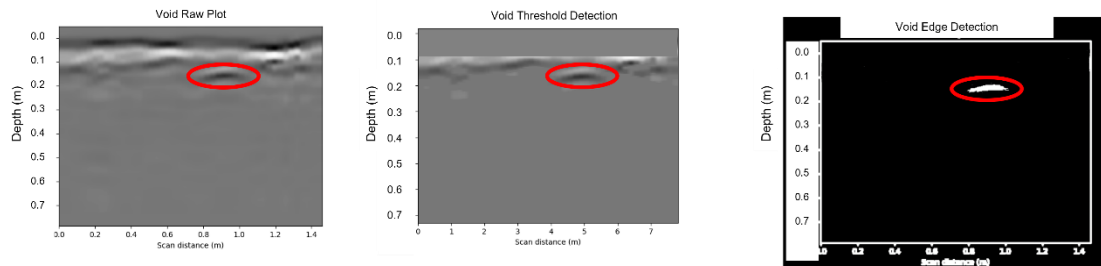


Figure 12. Void anomaly: Aug16_void6

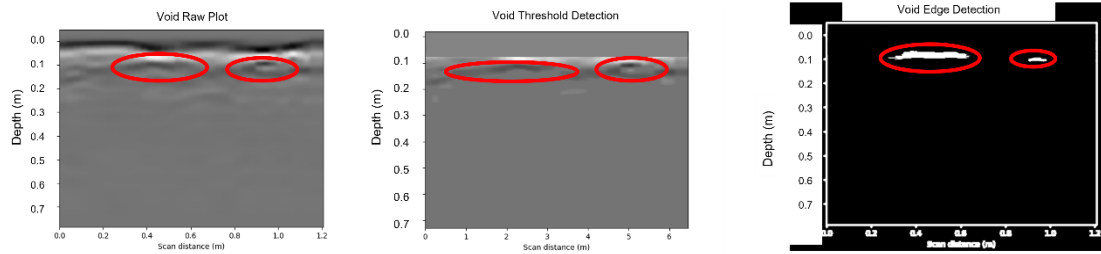


Figure 13. Void anomaly: Aug16_void12

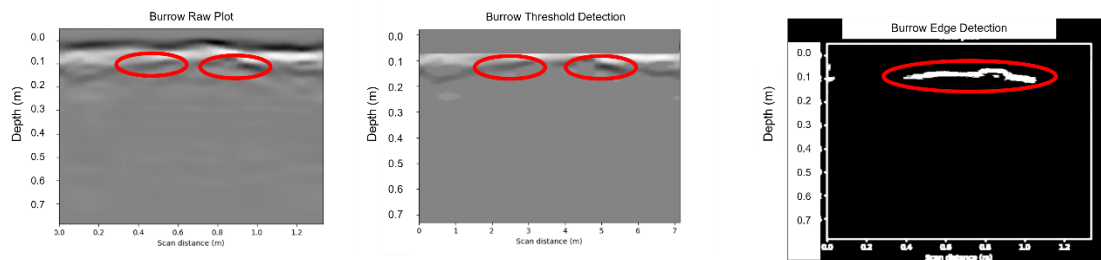


Figure 14. Animal burrow anomaly: Aug16_burrow3

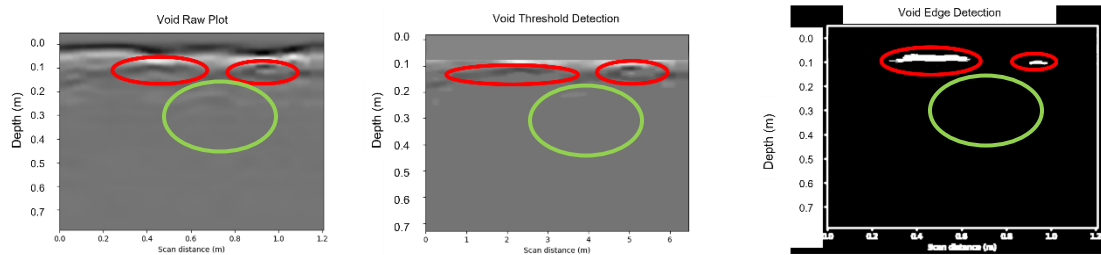


Figure 15. Animal burrow anomaly: Aug16_burrow6_surface

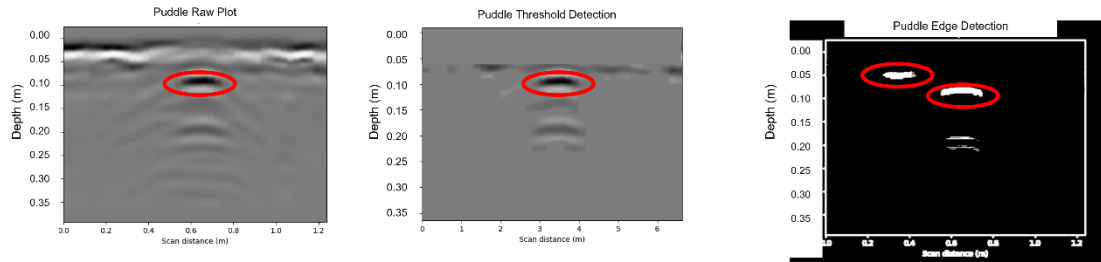


Figure 16. Water accumulation anomaly: Aug16_puddle_surface

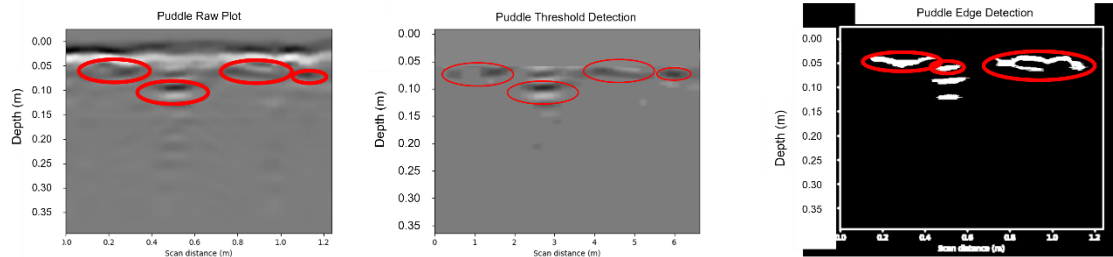


Figure 17. Water accumulation anomaly: Aug16_puddle3

Both threshold detection and edge detection can remove some noise from the original B-Scan images, thus giving better visualization. However, more potential anomalies were circled out when using these detection methods. That is because we can reasonably assume that some of the reflections are part of the air-soil-interface. Thus, we can exclude them empirically. However, in threshold and edge detection, we want to remove the air-soil-interface, but due to the limitation of the current threshold detection and edge detection algorithms, the interface is not removed completely. So, since some reflections neither got removed nor can be related to the interface empirically, they must be counted as potential anomalies.

Table 4 shows some metrics for the threshold detection performance. It shows the detectability, i.e., how many of the actual anomalies are detected, the false positive rate and false negative rates.

Table 4. Detectability and the false alarm rates for detection

Detection Method	Detectability	False Positive	False Negative
Threshold Detection 80%	88.89 (8 out of 9)	47.06 (8 out of 17)	11.11 (1 out of 9)
Threshold Detection 90%	77.78 (7 out of 9)	0 (0 out of 17)	22.22 (2 out of 9)

As shown in Table 4, an 80% threshold level resulted in a significant percentage (8 out of 17) false positives. On the other hand, a 90% threshold level results in two missed anomalies. Thus, it might be inferred that an optimal threshold should be between 80% and 90% in this case. However, more data and tests might be required to ascertain this optimal value. A better approach might be to implement an adaptive threshold that could change for different B-Scans, according to a given criteria, which could best eliminate noise, while preserving necessary information.

DISCUSSION

From the results in Table 4, the CNN models do not have the best classification accuracy as compared to other prior NN models. That might be because some data was collected having different GPR step sizes. B-Scan images taken in the laboratory setup had the step size of 0.0069 meters, but new B-Scan taken in the field had step sized of 0.00323 meters. This generated a resolution difference in the B-Scan images. As more data is taken with the same resolution, the classification accuracy of the CNN model may increase. Other prior models (NN) display satisfactory results. However, one disadvantage of NN models is that they require manual extraction and preparation of the features. This process is non-trivial and time consuming and requires a skilled operator. On the contrary, CNN models, which take a whole B-Scan image as input, can be automated for simple and easy processing.

CONCLUSION

Machine learning algorithms are a useful tool that may be used to classify anomalies in closed CCR disposal sites. GPR and machine learning algorithms can be integrated for enhancing the integrity of a fly ash landfill site cap system by streamlining the inspection data processing. Further research is required for determining the best options for detecting and classifying GPR inspection data.

FUTURE STEPS

Collect negative data samples (B-Scan images without anomalies). The current model will always predict one anomaly type, no matter whether anomaly exist. To address the issue, negative samples need to be collected and fed into the model so that the model can give out "No anomaly" result.

Collect more data points. Data at different resolution, locations, times, and soil conditions are beneficial. The inclusion of images from various locations and conditions can make the model more robust. Real world anomalies can be very different from the experimental anomalies set up. Actual anomalies will help the algorithm in field testing.

Develop adaptive threshold level to best detect anomalies and reduce false alarm rates.

ACKNOWLEDGEMENT:

The authors acknowledge funding and support from the Electric Power Research Institute and American Electric Power.

REFERENCES

- [1] H. Gu, W. Villarroel, B. Gallagher, and B. Palmer, "Use of machine learning algorithms to classify anomalies in closed CCR disposal sites", Technical Poster, World of Coal Ash Conference, May 16, 2022. Covington, KY.
- [2] Ohio Environmental Protection Agency Division of Environmental Response and Revitalization, "Closure plan review guidance for RCRA facilities," Dec, 2021.
- [3] A. N. Pankhej Bhojchand, "Signal processing algorithms to enhance detection of subsurface anomalies using GPR." OSU ECE Internal Report, Apr. 2020.
- [4] A. Benedetto and F. Benedetto, "13.15 - application Field-Specific synthesizing of sensing technology: Civil engineering application of ground-penetrating radar sensing technology," in Comprehensive Materials Processing, S. Hashmi et al, Ed. 2014, Available: <https://www.sciencedirect.com/science/article/pii/B9780080965321013157>. DOI: <https://doi.org/10.1016/B978-0-08-096532-1.01315-7>.
- [5] (Mar 21,). Permittivity of some common materials. Available: [https://eng.libretexts.org/Bookshelves/Electrical_Engineering/Electro-Optics/Book%3A_Electromagnetics_I_\(Ellingson\)/10%3A_Appendices/10.01%3A_Permittivity_of_Some_Common_Materials](https://eng.libretexts.org/Bookshelves/Electrical_Engineering/Electro-Optics/Book%3A_Electromagnetics_I_(Ellingson)/10%3A_Appendices/10.01%3A_Permittivity_of_Some_Common_Materials).
- [6] W. Marais et al, "Leveraging spatial textures, through machine learning, to identify aerosols and distinct cloud types from multispectral observations," Atmospheric Measurement Techniques, vol. 13, pp. 5459-5480, 2020. . DOI: 10.5194/amt-13-5459-2020.
- [7] Zhongming Xiang, Abbas Rashidi and Ge Ou, "An improved convolutional neural network system for automatically detecting rebar in GPR data," in ASCE International Conference on Computing in Civil Engineering 2019, Jun 13, 2019.
- [8] Laith Alzubaidi et al, "Review of deep learning: concepts, CNN architectures, challenges, applications, future directions," Journal of Big Data, vol. 8, (1), 2021. Available: <https://www.proquest.com/docview/2507363662?pq-origsite=gscholar&fromopenview=true>.
- [9] H. Yen, "The effect of normalization on the accuracy of data classification using neural networks," OSU ECE Internal Report, Apr. 2021.
- [10] A. Justin, "Image- and signal-based models for classification of subsurface anomalies using a ground penetrating radar," OSU ECE Internal Report, Apr. 2021.
- [11] S. Ghosh, "Edge and threshold detection," OSU ECE Internal Report, Nov. 2021.